Editors' Suggestion

Power-Law Density of States in Organic Solar Cells Revealed by the Open-Circuit Voltage Dependence of the Ideality Factor

Maria Saladina,[1,*] Christopher Wöpke,[1] Clemens Göhler,[1] Ivan Ramirez,[2] Olga Gerdes,[2] Chao Liu,[3,4] Ning Li,[3,4,5] Thomas Heumüller,[3,4] Christoph J. Brabec,[3,4] Karsten Walzer,[2] Martin Pfeiffer,[2] and Carsten Deibel[1,†]

[1]*Institut für Physik, Technische Universität Chemnitz, 09126 Chemnitz, Germany*
[2]*Heliatek GmbH, 01139 Dresden, Germany*
[3]*Institute of Materials for Electronics and Energy Technology (i-MEET), Friedrich-Alexander-Universität Erlangen-Nürnberg, 91054 Erlangen, Germany*
[4]*Helmholtz Institute Erlangen-Nürnberg for Renewable Energy (HI ERN), 91058 Erlangen, Germany*
[5]*State Key Laboratory of Luminescent Materials and Devices, Institute of Polymer Optoelectronic Materials and Devices, School of Materials Science and Engineering, South China University of Technology, 510640 Guangzhou, China*

(Received 13 July 2022; revised 27 February 2023; accepted 13 April 2023; published 9 June 2023)

The density of states (DOS) is fundamentally important for understanding physical processes in organic disordered semiconductors, yet hard to determine experimentally. We evaluated the DOS by considering recombination via tail states and using the temperature and open-circuit voltage (V_{oc}) dependence of the ideality factor. By performing Suns-V_{oc} measurements, we find that the energetic disorder increases deeper into the band gap, which is not expected for a Gaussian or exponential DOS. The linear dependence of the disorder on energy reveals the power-law DOS in organic solar cells.

DOI: 10.1103/PhysRevLett.130.236403

The dominant recombination mechanism in a solar cell is intimately related to the ideality factor [1–3]. For inorganic semiconductors, the closer the ideality factor gets to 2, the more dominant the share of trap-assisted recombination [4]. This connection is more complex for organic materials used in the state-of-the-art solar cells due to the energetic disorder inherent to these systems, giving rise to wave function localization. Consequently, charge carrier transport and recombination in these disordered materials strongly depend on the energetic distribution of localized states [5–9]. If the density of states (DOS) can be approximated by a Gaussian, the ideality factor becomes unity and independent of temperature [9,10]. However, temperature-independent ideality factors equal to 1 are yet to be reported for organic donor-acceptor systems [11–14], implying that the DOS is more complicated in these materials [15–17].

In this Letter, we seek to unravel the real shape of the DOS in a set of solar cells based on organic semiconductor blends. To achieve this aim, we determine ideality factors from temperature-dependent Suns-V_{oc} measurements. We connect the results to theoretical predictions by the multiple-trapping-and-release (MTR) model [7,8,18,19], using different combinations of the Gaussian and exponential DOS functions [20–25] to describe the energetic state distribution of electrons and holes. Depending on the shape of the DOS and the dominant recombination mechanism, the temperature dependence of the ideality factor differs [9], which allows us to assign specific recombination models to the investigated systems. We find that the characteristic energy of the DOS distribution in these organic solar cells depends on the energetic position within the DOS, resulting in a power-law distribution of localized states.

Current-voltage characteristics of a solar cell are usually approximated by the diode equation [26]. The recombination rate R enters the diode equation via recombination current density j_{rec}, which at the open-circuit conditions takes the form [27]

$$j_{rec} = e\int_0^L R(x)dx \approx eLR = j_0 \exp\left(\frac{eV_{oc}}{n_{id}k_BT}\right). \quad (1)$$

Here L stands for the active layer thickness, j_0 is the dark saturation current density, n_{id} is the ideality factor, V_{oc} is the open-circuit voltage, e is the elementary charge, k_B is the Boltzmann constant, and T is the temperature. To determine the DOS, we evaluate the dependence of n_{id} on R.

In organic disordered materials, the localized states in the DOS that lie below the transport energy act as traps, which capture mobile charge carriers [28]. Trapped charge carriers can be thermally released and contribute to photoconductivity. During this process of multiple trapping and release [7,8,18,19], some share of charge carriers recombines and is lost to the photocurrent. In the MTR model, the

fraction of the mobile charge carrier density is expressed through parameter θ, the trapping factor, which depends on the DOS distribution [7,19,29]. The density of mobile and trapped charge carriers is expressed as $n_c = \theta n$ and $n_t = (1-\theta)n$, respectively, with $\theta \leq 1$. As the density of trapping states is much larger than the charge carrier density, most relaxed charge carriers populate energy sites in the DOS tail [30]. Thus, $n_c \ll n_t \approx n$ and $\theta \ll 1$, inferring that recombination is mainly trap mediated. Noting that, due to the nature of photogeneration, $n = p$, the recombination rate becomes

$$\begin{aligned} R &\approx k_{r,n} n_c p_t + k_{r,p} n_t p_c \\ &\approx (k_{r,n}\theta_n + k_{r,p}\theta_p) n^2. \end{aligned} \tag{2}$$

Here k_r stands for the recombination prefactor, and the subscript denotes which of the charge carriers, electrons n or holes p, are mobile. The finite escape probability from the charge-transfer state back to the separated state, if present, is included in k_r and reduces it compared to the Langevin prefactor $k_L = e(\mu_n + \mu_p)/\varepsilon$ [31–33]. Additionally, k_r contains the effect of active layer morphology that causes its further deviation from k_L [34–37].

The two recombination channels in Eq. (2) are distinguished by the type of mobile charge carrier. One of the channels is dominant if its recombination prefactor and/or its trapping factor is larger than for the other channel. Thus, the exact expression of R depends on (i) the physical parameters, e.g., mobility, of the mobile charge carrier type through the recombination prefactor k_r, (ii) the DOS of this charge carrier type through the trapping factor θ, and (iii) the DOS of both charge carriers involved in the dominant recombination channel through the total charge carrier concentration n.

To determine and evaluate n_{id}, we focus on the most prevalent models used to approximate the DOS distributions in organic semiconductors—the Gaussian and exponential DOS [20–25]. The depth of trap states depends on the characteristic energy, i.e., the disorder parameter σ and the Urbach energy E_U, respectively. The resulting form of Eq. (2) is defined by four combinations of these DOS distributions [see Supplemental Material Eqs. (S11)–(S14) [38]]. For the detailed derivation, the interested reader is referred to the comprehensive work of Hofacker and Neher [9]. Here, we build on a mere fraction of their results related to the ideality factor and summarize relevant parts of the derivation in the Supplemental Material [38]. The ideality factor is obtained by comparing Eq. (1) to the equations of R for the DOS combinations discussed above.

Without loss of generality, we describe the dominant recombination channel involving mobile holes recombining with trapped electrons. The trapped electrons in the recombination channel ($n_t \approx n$) control the temperature dependence of the ideality factor, while the mobile holes ($p_c = \theta_p p$) control the recombination order. If the DOS of electrons is described by a Gaussian, in the low concentration limit we arrive at $n_{\mathrm{id}} = 1$, independent of temperature [9,10,40]. This is true irrespective of whether mobile holes come from the Gaussian or exponential DOS. An ideality factor of unity, however, is not observed experimentally in organic semiconductors [11–14].

In contrast, if the DOS of trapped electrons is exponential, the ideality factor is temperature dependent. When such electrons recombine with mobile holes from a Gaussian DOS, the ideality factor is independent of σ and is expressed as [9]

$$n_{\mathrm{id}} = \frac{E_U + k_B T}{2 k_B T}. \tag{3}$$

If mobile holes are also represented by an exponential DOS, the ideality factor is given by [9,12,41,42]

$$n_{\mathrm{id}} = \frac{2E_U}{E_U + k_B T}. \tag{4}$$

We refer to these models as the "mixed DOS" and "exponential DOS," respectively. In order to shed light on the shape of the DOS in organic materials, our focus lies on the temperature dependence of the ideality factor, with the models underlying Eqs. (3) and (4) as the starting point.

To verify that the DOS can be established through ideality factors, we chose the well-studied hydrogenated amorphous silicon solar cell as a reference due to its exponential DOS. We then expanded our investigation to a set of material systems representative of typical organic solar cell classes, such as solution-processed fullerene (P3HT:$PC_{61}BM$) and nonfullerene acceptor devices (PM6:Y6), along with thermally evaporated small-molecule solar cells (DCV-V-Fu-Ind-Fu-V:C_{60}). The details of molecular structure and device fabrication are given in the Supplemental Material [38].

We employ illumination intensity-dependent V_{oc} measurements to determine ideality factors in the absence of series and transport resistance [43–45]. Figure 1(a) shows the Suns-V_{oc} data of an a-Si:H solar cell between 150 and 300 K. The regions of low light intensity are influenced by low shunt resistance. Roughly above 1 sun, V_{oc} becomes limited by the contacts, which is more pronounced at low temperatures. Ideality factors were extracted from the slope of $\Phi(V_{\mathrm{oc}})$ according to [13]

$$n_{\mathrm{id}} = \frac{e}{k_B T}\left(\frac{d\ln\Phi}{dV_{\mathrm{oc}}}\right)^{-1}. \tag{5}$$

For each temperature, the data can be fitted with a single slope over 2 orders of magnitude of light intensities.

We show the resulting ideality factors as a function of the inverse temperature in Fig. 1(b). Consistent with van Berkel *et al.* [41], we observe the decrease of n_{id} of the a-Si:H solar

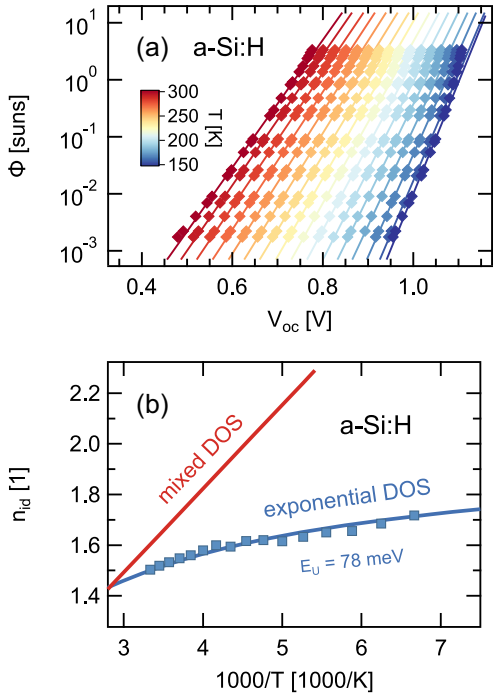

FIG. 1. (a) Suns-V_{oc} data (symbols) of a-Si:H solar cell fitted with Eq. (5) (solid lines). (b) Temperature-dependent ideality factor n_{id} extracted from the fits in comparison to Eqs. (3) and (4).

cell with higher temperature from 1.7 at 150 K to 1.5 at 300 K. The temperature dependence of n_{id} can be fitted with Eq. (4) and therefore is assigned to the trap-assisted recombination of charge carriers within the exponential density of states. The fit yields the Urbach energy of ≈78 meV, in agreement with the literature [41,46], which is independent of temperature and light intensity. In the exponential DOS model $n_{id} \propto (E_U + k_B T)^{-1}$, resulting in a sublinear dependence on $1/T$. A mixed DOS would lead to a distinctly different temperature dependence of the ideality factor, as $n_{id} \propto 1/T$ according to Eq. (3).

We now extend the scope of the study to organic donor-acceptor systems. Figure 2 shows ideality factors of P3HT:$PC_{61}BM$, PM6:Y6, and DCV-V-Fu-Ind-Fu-V:C_{60}. First, we note that, at each temperature, n_{id} has several values corresponding to the local slope of $\Phi(V_{oc})$. Hence, in contrast to a-Si:H, the ideality factor of the organic systems we investigate here is light intensity dependent and generally decreases with increasing light intensity. Initially, it seems problematic to assign a specific recombination model based on the temperature dependence of n_{id} at a certain illumination intensity (cf. Supplemental Material Fig. S05 [38]). The position within the DOS depends on both temperature and illumination intensity. For a fixed range of illumination intensities, at lower temperatures we probe states closer to the effective band gap, as compared to higher temperatures. If the DOS of trapped charge carriers is not strictly exponential, its characteristic energy changes with the quasi-Fermi level splitting (QFLS), something not accounted for by the method.

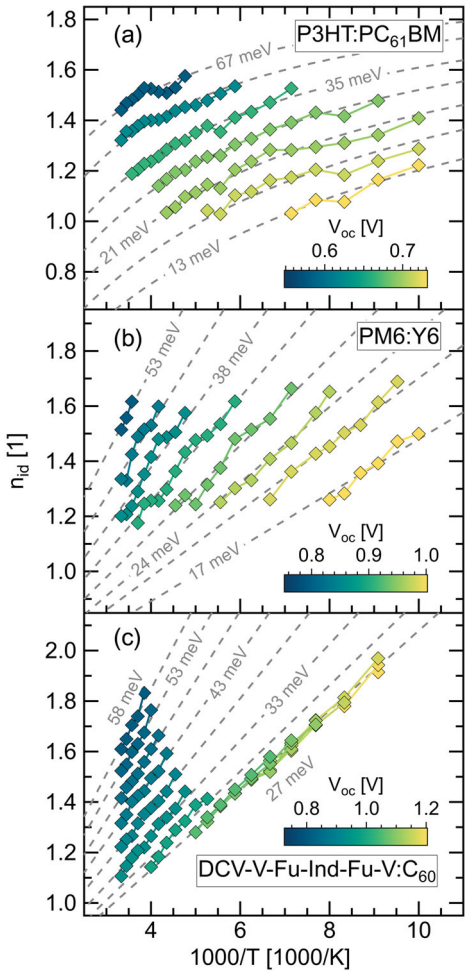

FIG. 2. Temperature-dependent ideality factors n_{id} of (a) P3HT:$PC_{61}BM$, (b) PM6:Y6, and (c) DCV-V-Fu-Ind-Fu-V:C_{60} (symbols). Darker color corresponds to lower V_{oc}, i.e., deeper subgap energy states. Dashed lines are the calculated $n_{id}(E_U, T)$ according to Eq. (4) for P3HT:$PC_{61}BM$ and Eq. (3) for PM6:Y6 and DCV-V-Fu-Ind-Fu-V:C_{60}. E_U increases with the DOS depth for all three systems.

Instead, we evaluate the data at fixed V_{oc} (cf. Fig. S06 [38]). The QFLS, approximated by V_{oc}, samples the combined DOS of electrons and holes at a certain energy. The Urbach energy, which is a measure of disorder for the exponential DOS distribution, is independent of temperature at fixed V_{oc}, and the ideality factor describes the dominant recombination mechanism at this DOS depth. Coming back to Fig. 2, we see our approach paying off. For a given V_{oc}, the relation between n_{id} and $1/T$ can be assigned to specific recombination models for all three material systems. Ideality factors of P3HT:$PC_{61}BM$ in Fig. 2(a) at a given V_{oc} follow the exponential DOS model (4), similar to what we found for a-Si:H earlier. PM6:Y6 and DCV-V-Fu-Ind-Fu-V:C_{60} in Figs. 2(b) and 2(c), on the other hand, are best described by the mixed DOS model (3).

We calculate n_{id} using different values of E_U (indicated by dashed lines in the figure) and find good agreement with

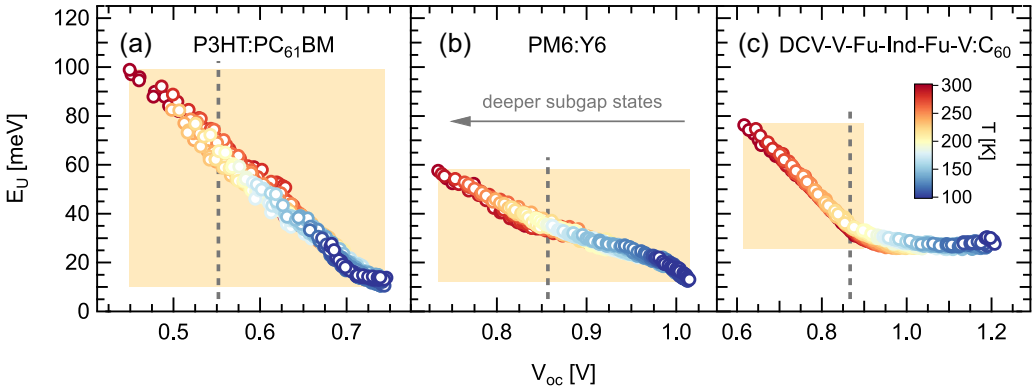

FIG. 3. Urbach energies E_U as a function of the quasi-Fermi level splitting, approximated by V_{oc}. E_U was calculated from $n_{id}(T)$ according to Eq. (4) for (a) P3HT:PC_{61}BM and Eq. (3) for (b) PM6:Y6 and (c) DCV-V-Fu-Ind-Fu-V:C_{60}. E_U is independent of T, while it depends linearly on V_{oc} within the highlighted areas, inferring that the DOS is described by a power law. Roughly constant E_U outside of the highlighted area is an indication of the exponential DOS. Dashed lines correspond to V_{oc} at 1 sun illumination intensity at room temperature.

the data. For a strictly exponential DOS, the Urbach energy is constant and describes the DOS globally. For all three organic donor-acceptor systems, however, the Urbach energy describes the DOS of trapped charge carriers only locally and becomes a function of energy, inferring that the exponential DOS acts as a local approximation of the real DOS at a given QFLS [16]. The deeper we are probing in the density of states, the larger the E_U. The DOS of the thermally evaporated DCV-V-Fu-Ind-Fu-V:C_{60} solar cell is nearly exponential above 0.90 V, as E_U is roughly constant in this region.

Figure 3 shows the relation between the Urbach energy and the QFLS. First, we note a striking convergence of E_U at different temperatures for all the systems, strengthening our confidence in the analytical approach and the assigned system-specific recombination models. E_U depends linearly on the QFLS in the regions of nonconstant Urbach energy (highlighted areas in the figure). This linearity helps to unravel the real shape of the density of states. For the exponential DOS $g_{exp}(E)$,

$$\frac{d \ln g_{exp}(E)}{dE} = \frac{1}{E_U}. \tag{6}$$

We emphasize again that in our case the exponential function acts as a local approximation of the real DOS. With the linear relation that we observe, $E_U(E) = (E - E_0)/\xi$, the derivative of the real DOS distribution is given by

$$\frac{d \ln g(E)}{dE} = \frac{\xi}{E - E_0}. \tag{7}$$

This relation leads to $\ln g(E) \propto \xi \ln (E - E_0)$, and the ultimate form of the DOS distribution is a power law,

$$g(E) \propto (E - E_0)^{\xi}. \tag{8}$$

To our knowledge, the power-law density of states has not been reported for organic solar cells before. However, it must be considered when explaining experimental data and simulating the physics of organic semiconductors, as we observe this DOS distribution in all the donor-acceptor systems investigated herein. The power-law DOS can be assigned to P3HT:PC_{61}BM and PM6:Y6 in the whole measured data range. The density of states of DCV-V-Fu-Ind-Fu-V:C_{60} follows the power law up to ca. 0.90 V and changes its shape to exponential at higher V_{oc}. Compared to an exponential DOS, the power law is described by a narrower tail. Hence, there are fewer available states for the charge carriers to fill up, resulting in a higher V_{oc} than would be expected for the exponential DOS. By averaging, we find that under 1 sun illumination at room temperature $E_U \approx 66$ meV for P3HT:PC_{61}BM, similar to previous reports [12,42,47]. In DCV-V-Fu-Ind-Fu-V:C_{60} and PM6:Y6, the energetic disorder is reduced ($E_U \approx 35$ meV) [48–50], and the trap distribution is narrower compared to P3HT:PC_{61}BM. Lower disorder is, in general, beneficial to the solar cell performance, as it leads to enhanced charge carrier transport and reduced V_{oc} losses [51–53].

In conclusion, we employ temperature and illumination intensity-dependent V_{oc} measurements to determine the type of the density of states in PM6:Y6, DCV-V-Fu-Ind-Fu-V:C_{60}, and P3HT:PC_{61}BM organic solar cells. We find that the temperature dependence of the ideality factor can be explained in the framework of the multiple-trapping-and-release model, but only if analyzed at a given open-circuit voltage. For all the investigated organic systems, the density of states of trapped charge carriers participating in recombination is locally approximated by the exponential one, where the characteristic energy of the distribution decreases linearly with increasing quasi-Fermi level splitting. Our results establish that the density of states

in these solar cells follows a power law, which has not been reported for organic donor-acceptor systems up to date. We suggest that the temperature-dependent experiments designed to understand recombination mechanisms in these disordered systems have to be conducted at the same quasi-Fermi level splitting to ensure correct interpretation of the results.

The authors are grateful to J. Gorenflot, KAUST, for his valuable comments on the Letter. We thank the Deutsche Forschungsgemeinschaft (DFG) for funding this work (Research Unit FOR 5387 POPULAR, Project No. 461909888).

*maria.saladina@physik.tu-chemnitz.de
†deibel@physik.tu-chemnitz.de

[1] G. A. H. Wetzelaer, M. Kuik, H. T. Nicolai, and P. W. M. Blom, Phys. Rev. B **83**, 165204 (2011).
[2] C. Göhler, A. Wagenpfahl, and C. Deibel, Adv. Electron. Mater. **4**, 1700505 (2018).
[3] W. Tress, M. Yavari, K. Domanski, P. Yadav, B. Niesen, J. P. C. Baena, A. Hagfeldt, and M. Graetzel, Energy Environ. Sci. **11**, 151 (2018).
[4] C.-T. Sah, R. N. Noyce, and W. Shockley, Proc. IRE **45**, 1228 (1957).
[5] H. Bässler, Phys. Status Solidi (b) **175**, 15 (1993).
[6] O. Rubel, S. D. Baranovskii, P. Thomas, and S. Yamasaki, Phys. Rev. B **69**, 014206 (2004).
[7] S. Baranovskii, Phys. Status Solidi (b) **251**, 487 (2014).
[8] A. Nenashev, J. Oelerich, and S. Baranovskii, J. Phys. Condens. Matter **27**, 093201 (2015).
[9] A. Hofacker and D. Neher, Phys. Rev. B **96**, 245204 (2017).
[10] J. C. Blakesley and D. Neher, Phys. Rev. B **84**, 075210 (2011).
[11] R. A. Street, A. Krakaris, and S. R. Cowan, Adv. Funct. Mater. **22**, 4608 (2012).
[12] A. Foertig, J. Rauh, V. Dyakonov, and C. Deibel, Phys. Rev. B **86**, 115302 (2012).
[13] K. Tvingstedt and C. Deibel, Adv. Energy Mater. **6**, 1502230 (2016).
[14] L. Perdigón-Toro, L. Q. Phuong, F. Eller, G. Freychet, E. Saglamkaya, J. I. Khan, Q. Wei, S. Zeiske, D. Kroh, S. Wedler, A. Köhler, A. Armin, F. Laquai, E. M. Herzig, Y. Zou, S. Shoaee, and D. Neher, Adv. Energy Mater. **12**, 2103422 (2022).
[15] R. C. MacKenzie, T. Kirchartz, G. F. Dibb, and J. Nelson, J. Phys. Chem. C **115**, 9806 (2011).
[16] R. C. MacKenzie, C. G. Shuttle, M. L. Chabinyc, and J. Nelson, Adv. Energy Mater. **2**, 662 (2012).
[17] J. O. Oelerich, D. Huemmer, and S. D. Baranovskii, Phys. Rev. Lett. **108**, 226403 (2012).
[18] J. Noolandi, Phys. Rev. B **16**, 4466 (1977).
[19] V. Arkhipov, V. Kolesnikov, and A. Rudenko, J. Phys. D **17**, 1241 (1984).
[20] P. Mark and W. Helfrich, J. Appl. Phys. **33**, 205 (1962).
[21] G. Paasch and S. Scheinert, J. Appl. Phys. **107**, 104501 (2010).
[22] G. Garcia-Belmonte, Sol. Energy Mater. Sol. Cells **94**, 2166 (2010).
[23] T. Kirchartz and J. Nelson, Phys. Rev. B **86**, 165201 (2012).
[24] T. M. Burke, S. Sweetnam, K. Vandewal, and M. D. McGehee, Adv. Energy Mater. **5**, 1500123 (2015).
[25] B. Xiao, P. Calado, R. C. I. MacKenzie, T. Kirchartz, J. Yan, and J. Nelson, Phys. Rev. Appl. **14**, 024034 (2020).
[26] W. Shockley, Bell Syst. Tech. J. **28**, 435 (1949).
[27] U. Würfel, D. Neher, A. Spies, and S. Albrecht, Nat. Commun. **6**, 6951 (2015).
[28] V. I. Arkhipov, E. V. Emelianova, and G. J. Adriaenssens, Phys. Rev. B **64**, 125125 (2001).
[29] G. J. Adriaenssens, S. D. Baranovskii, W. Fuhs, J. Jansen, and Ö. Öktü, Phys. Rev. B **51**, 9661 (1995).
[30] V. Arkhipov, I. Fishchuk, A. Kadashchuk, and H. Bässler, Charge transport in disordered organic semiconductors, in *Photophysics of Molecular Materials: From Single Molecules To Single Crystals* (Wiley-VCH Verlag, Weinheim, 2006), Chap. 6, pp. 261–366, 10.1002/3527607323.ch6.
[31] P. Langevin, Ann. Chim. Phys. **28**, 433 (1903).
[32] C. L. Braun, J. Chem. Phys. **80**, 4157 (1984).
[33] S. Shoaee, A. Armin, M. Stolterfoht, S. M. Hosseini, J. Kurpiers, and D. Neher, Solar RRL **3**, 1900184 (2019).
[34] L. Koster, V. Mihailetchi, and P. Blom, Appl. Phys. Lett. **88**, 052104 (2006).
[35] J. Gorenflot, M. C. Heiber, A. Baumann, J. Lorrmann, M. Gunz, A. Kämpgen, V. Dyakonov, and C. Deibel, J. Appl. Phys. **115**, 144502 (2014).
[36] M. C. Heiber, C. Baumbach, V. Dyakonov, and C. Deibel, Phys. Rev. Lett. **114**, 136602 (2015).
[37] M. C. Heiber, T.-Q. Nguyen, and C. Deibel, Phys. Rev. B **93**, 205204 (2016).
[38] See Supplemental Material at http://link.aps.org/supplemental/10.1103/PhysRevLett.130.236403 for experimental methods, details of the theoretical model, and data analysis, which includes Ref. [39].
[39] R. Fitzner, E. Mena-Osteritz, A. Mishra, G. Schulz, E. Reinold, M. Weil, C. Körner, H. Ziehlke, C. Elschner, K. Leo, M. Riede, M. Pfeiffer, C. Uhrich, and P. Bäuerle, J. Am. Chem. Soc. **134**, 11064 (2012).
[40] W. F. Pasveer, J. Cottaar, C. Tanase, R. Coehoorn, P. A. Bobbert, P. W. M. Blom, D. M. de Leeuw, and M. A. J. Michels, Phys. Rev. Lett. **94**, 206601 (2005).
[41] C. van Berkel, M. Powell, A. Franklin, and I. French, J. Appl. Phys. **73**, 5264 (1993).
[42] T. Kirchartz, B. E. Pieters, J. Kirkpatrick, U. Rau, and J. Nelson, Phys. Rev. B **83**, 115209 (2011).
[43] M. Wolf and H. Rauschenbach, Adv. Energ. Convers. **3**, 455 (1963).
[44] T. Kirchartz, F. Deledalle, P. S. Tuladhar, J. R. Durrant, and J. Nelson, J. Phys. Chem. Lett. **4**, 2371 (2013).
[45] C. Wöpke *et al.*, Nat. Commun. **13**, 3786 (2022).
[46] R. Wehrspohn, S. Deane, I. French, I. Gale, J. Hewett, M. Powell, and J. Robertson, J. Appl. Phys. **87**, 144 (2000).
[47] B. Jarzkąbek, P. Nitschke, B. Hajduk, M. Domański, and H. Bednarski, Polymer Test. **88**, 106573 (2020).
[48] A. Karki, J. Vollbrecht, A. L. Dixon, N. Schopp, M. Schrock, G. M. Reddy, and T.-Q. Nguyen, Adv. Mater. **31**, 1903868 (2019).

[49] J. Wu, J. Lee, Y.-C. Chin, H. Yao, H. Cha, J. Luke, J. Hou, J.-S. Kim, and J. R. Durrant, Energy Environ. Sci. **13**, 2422 (2020).
[50] T. Yang, R. Ma, H. Cheng, Y. Xiao, Z. Luo, Y. Chen, S. Luo, T. Liu, X. Lu, and H. Yan, J. Mater. Chem. A **8**, 17706 (2020).
[51] I. Lange, J. Kniepert, P. Pingel, I. Dumsch, S. Allard, S. Janietz, U. Scherf, and D. Neher, J. Phys. Chem. Lett. **4**, 3865 (2013).
[52] S. D. Collins, C. M. Proctor, N. A. Ran, and T.-Q. Nguyen, Adv. Energy Mater. **6**, 1501721 (2016).
[53] C. Göhler and C. Deibel, ACS Energy Lett. **7**, 2156 (2022).